General Disclaimer

One or more of the Following Statements may affect this Document

- This document has been reproduced from the best copy furnished by the organizational source. It is being released in the interest of making available as much information as possible.

- This document may contain data, which exceeds the sheet parameters. It was furnished in this condition by the organizational source and is the best copy available.

- This document may contain tone-on-tone or color graphs, charts and/or pictures, which have been reproduced in black and white.

- This document is paginated as submitted by the original source.

- Portions of this document are not fully legible due to the historical nature of some of the material. However, it is the best reproduction available from the original submission.

Produced by the NASA Center for Aerospace Information (CASI)

NATIONAL AERONAUTICS AND SPACE ADMINISTRATION

Technical Memorandum 33-775

Low Work Function Silicon Collector for Thermionic Converters

(NASA-CR-147947) LOW WORK FUNCTION SILICON COLLECTOR FOR THERMIONIC CONVERTERS (Jet Propulsion Lab.) 34 p HC $4.00 CSCL 10A

N76-23704

Unclas
G3/44 28209

JET PROPULSION LABORATORY
CALIFORNIA INSTITUTE OF TECHNOLOGY
PASADENA, CALIFORNIA

May 15, 1976

JUN 1976
RECEIVED
NASA STI FACILITY
INPUT BRANCH

TECHNICAL REPORT STANDARD TITLE PAGE

1. Report No. 33-775	2. Government Accession No.	3. Recipient's Catalog No.
4. Title and Subtitle LOW WORK FUNCTION SILICON COLLECTOR FOR THERMIONIC CONVERTERS		5. Report Date May 15, 1976 6. Performing Organization Code
7. Author(s) K. H. Chang, K. Shimada		8. Performing Organization Report No.
9. Performing Organization Name and Address JET PROPULSION LABORATORY California Institute of Technology 4800 Oak Grove Drive Pasadena, California 91103		10. Work Unit No. 11. Contract or Grant No. NAS 7-100 13. Type of Report and Period Covered Technical Memorandum
12. Sponsoring Agency Name and Address NATIONAL AERONAUTICS AND SPACE ADMINISTRATION Washington, D.C. 20546		14. Sponsoring Agency Code

15. Supplementary Notes

16. Abstract

To improve the efficiency of present thermionic converters, single crystal silicon was investigated as a low work function collector material. The experiments were conducted in a test vehicle which resembled an actual thermionic converter.

The test vehicle was constructed from standard stainless steel vacuum components incorporating facilities to sputter clean the collector surface, activate it and monitor the progress of activation. The (100) oriented silicon single crystal wafers were diffusion bonded on molybdenum blocks to form collectors. The silicon surface was activated by cesium and oxygen after careful in-situ preparation of the surface.

Work function as low as 1.0eV was obtained with an n-type silicon. The stabilities of the activated surfaces at elevated temperatures were tested by raising the collector temperature up to 829°K. By increasing the Cs arrival rate, it was possible to restore the originally activated low work function of the surface at elevated surface temperatures. These results plotted in the form of Rasor-Warner curve, have shown a behavior similar to that of metal electrode except that the minimum work function was much lower with silicon than with metals. It was also noted that the lowest work function reproduced at elevated temperatures was dependent upon the original

17. Key Words (Selected by Author(s))	18. Distribution Statement
Nonmetallic Materials Solid-State Physics	Unclassified -- Unlimited

19. Security Classif. (of this report)	20. Security Classif. (of this page)	21. No. of Pages	22. Price
Unclassified	Unclassified	29	

HOW TO FILL OUT THE TECHNICAL REPORT STANDARD TITLE PAGE

Make items 1, 4, 5, 9, 12, and 13 agree with the corresponding information on the report cover. Use all capital letters for title (item 4). Leave items 2, 6, and 14 blank. Complete the remaining items as follows:

3. Recipient's Catalog No. Reserved for use by report recipients.

7. Author(s). Include corresponding information from the report cover. In addition, list the affiliation of an author if it differs from that of the performing organization.

8. Performing Organization Report No. Insert if performing organization wishes to assign this number.

10. Work Unit No. Use the agency-wide code (for example, 923-50-10-06-72), which uniquely identifies the work unit under which the work was authorized. Non-NASA performing organizations will leave this blank.

11. Insert the number of the contract or grant under which the report was prepared.

15. Supplementary Notes. Enter information not included elsewhere but useful, such as: Prepared in cooperation with... Translation of (or by)... Presented at conference of... To be published in...

16. Abstract. Include a brief (not to exceed 200 words) factual summary of the most significant information contained in the report. If possible, the abstract of a classified report should be unclassified. If the report contains a significant bibliography or literature survey, mention it here.

17. Key Words. Insert terms or short phrases selected by the author that identify the principal subjects covered in the report, and that are sufficiently specific and precise to be used for cataloging.

18. Distribution Statement. Enter one of the authorized statements used to denote releasability to the public or a limitation on dissemination for reasons other than security of defense information. Authorized statements are "Unclassified—Unlimited," "U. S. Government and Contractors only," "U. S. Government Agencies only," and "NASA and NASA Contractors only."

19. Security Classification (of report). NOTE: Reports carrying a security classification will require additional markings giving security and downgrading information as specified by the Security Requirements Checklist and the DoD Industrial Security Manual (DoD 5220.22-M).

20. Security Classification (of this page). NOTE: Because this page may be used in preparing announcements, bibliographies, and data banks, it should be unclassified if possible. If a classification is required, indicate separately the classification of the title and the abstract by following these items with either "(U)" for unclassified, or "(C)" or "(S)" as applicable for classified items.

21. No. of Pages. Insert the number of pages.

22. Price. Insert the price set by the Clearinghouse for Federal Scientific and Technical Information or the Government Printing Office, if known.

PREFACE

The work described in this report was performed by the Guidance and Control Division of the Jet Propulsion Laboratory.

CONTENTS

Figure Captions

PRECEDING PAGE BLANK NOT FILMED

ABSTRACT

To improve the efficiency of present thermionic converters, single crystal silicon was investigated as a low work function collector material. The experiments were conducted in a test vehicle which resembled an actual thermionic converter.

The test vehicle was constructed from standard stainless steel vacuum components incorporating facilities to sputter clean the collector surface, activate it and monitor the progress of activation. The (100) oriented silicon single crystal wafers were diffusion bonded on molybdenum blocks to form collectors. The silicon surface was activated by cesium and oxygen after careful in-situ preparation of the surface.

Work function as low as 1.0eV was obtained with an n-type silicon. The stabilities of the activated surfaces at elevated temperatures were tested by raising the collector temperature up to 829°K. By increasing the Cs arrival rate, it was possible to restore the originally activated low work function of the surface at elevated surface temperatures. These results plotted in the form of Rasor-Warner curve, have shown a behavior similar to that of metal electrode except that the minimum work function was much lower with silicon than with metals. It was also noted that the lowest work function reproduced at elevated temperatures was dependent upon the original work function values obtained at room temperatures.

I. Introduction

Analysis of current state-of-the-art thermionic converters has indicated[1] that further improvements in conversion efficiencies of thermionic converters must arise from a decrease in collector work function and a reduction of the plasma voltage drop. The two phenomena are not totally independent of each other, but in large part, the problems can be separated.

The problem of reducing the work function has been extensively pursued, and values lower than 1.0 electron volts have been achieved in a number of metal-oxide-cesium systems[2] and semiconductor-cesium-oxygen systems[3, 4]. However, in thermionic converters collector work function values have been larger than 1.5eV.

Therefore, during the past few years, research has been in progress to develop a low work function collector which would be usable in a thermionic converter. If one can achieve a barrier index (sum of the collector work function and the plasma drop) of 1.2eV, a conversion efficiency at the electrodes as high as 29% can be achieved at an emitter temperature T_e of 1400°K as shown in Table I.

The purpose of the present study is to develop a low work function collector whose work function is less than 1.2eV, by adopting the techniques developed for photocathode materials. Among a few potential candidate materials such as metal-oxide-cesium and semiconductor-cesium-oxygen systems, silicon single crystals were chosen as the test collector material for investigation at JPL since the silicon (100) surface has already been successfully activated to work functions lower than 1.0eV and has been tested at elevated temperatures elsewhere[5]. Experimental results obtained from a number of collectors made from both n- and p-type silicon are presented in this paper.

Table I. Calculated Performance of High and Low Temperature Thermionic Converters

Variables			High Temp. Conv.	Advanced Conv.	Ideal Conv.
Emitter Temp.	T_e	(°K)	2000	1400	1400
Collector Temp.	T_c	(°K)	1000	700	700
Cesium Temp.	T_{Cs}	(°K)	600	400	400
Emitter Work Function	ϕ_e	(eV)	3.0	2.0	2.0
Collector Work Function	ϕ_c	(eV)	1.7	1.0	1.0
Plasma Drop	V_p	(V)	0.6	0.2	0
Output Volt.	V_o	(V)	0.6	0.8	1.0
Output Curr.	I_o	(A/cm^2)	12	14	14
Output Power	P_{OUT}	(W/cm^2)	8.4	11	14
Input Power	P_{IN}	(W/cm^2)	70	40	40
Efficiency	η	(%)	12	29	35

II. Experimental Apparatus

1. Test Vehicle

A schematic drawing of the test vehicle is shown in Figure 1. The envelope is made of a standard vacuum component, a 39-mm (1.5 inch) stainless steel "cross". A pair of opposite ports of the cross are used for the emitter and collector mountings; the remaining two ports are used for the vacuum pump connection and for an observation window. Two small tubes are welded at 45° angles to the wall of the cross in order to provide a port for an optical window and a port with a valve for the cesium supply. In addition, oxygen and argon supply lines are incorporated through a double flange at the observation window. The external view of the actual test vehicle is shown in Figure 2.

The emitter is made of a 90% transparent 100-mesh tungsten sheet screen, 25μm thick. An identical mesh, separated by 1.6mm, is provided so that it may be used as a grid electrode. Both the emitter and the grid can be directly heated by passing currents. The reason for both electrodes being transparent screens is that the sample collector surface must be in the line of sight from the optical window and the cesium tube for the introduction of cesium beam during experiments.

The collector assembly (Figure 3) is made of a 0.25mm thick silicon wafer bonded on a molybdenum block, and this assembly is surrounded by a molybdenum guard ring. The Si-Mo bonding was performed by heating them together in vacuum to approximately 1150°C. The bonding temperature was below the Si-Mo eutectic point (1400°C) and the Si surface visually maintained its original appearance after the bonding. The stress due to the thermal expansion mismatch causes the bond to break unless the rate of temperature variation is maintained at 10°C per minute or less.

The cesium reservoir is connected to the main chamber through a stainless steel valve, NUPRO Model 6BS-SW. The valve is open only during the period of cesiation. A heater wire is brazed onto the reservoir to control the cesium arrival rate at the Si electrode surface.

Reagent grade oxygen and argon sources are also incorporated in the test system. Oxygen is used as an activating agent for the test electrode; argon is used as the source of ions for sputter cleaning. These gases are contained in two glass flasks at one atmosphere pressure and are introduced to the system via precision flow control valves. The valve for the oxygen is a variable leak valve having a minimum leak rate of 1.3×10^{-8} N/m^2 liter per sec (1×10^{-10} Torr-liter/sec). The valve for argon is a micrometer controlled needle valve.

A sorption pump is provided for roughing the test vehicle and a 200 l/s ion pump is used to attain ultrahigh vacuum in a range of 10^{-8} N/m^2 (10^{-10} Torr). The pressure in the test chamber is estimated by reading the ion pump current and correcting for the conductance of the connecting tube.

2. Optical Monochromator

A simple and compact optical monochromator was designed for this experiment. It consisted of a 100 watt quartz-iodine tungsten lamp and a series of interchangeable interference filters. The optical design of the monochromator is shown in Figure 4. The lens L_1 is a condensor lens, which helps to form a uniform brightness distribution over the rectangular aperture area. L_2 and L_3 are a pair of matched lenses whose focal lengths are equal to d, the distance between the rectangular aperture and L_2. The optical rays which pass through the interference filter F perpendicularly form the image of the aperture on the target plane.

The light output of the monochromator was calibrated by using an Epply thermopile (SN #22489) in connection with a Keithley 149 millimicro voltmeter. A quartz window was used in front of the thermopile to reduce the noise due to air turbulence.

The transmission coefficients of the interference filters, procured from Optical Industries, Inc., Costa Mesa, California, were 50-65% with approximately 100Å pass bands.

The light output through a rectangular aperture of 0.282 cm^2 (4.44mm x 6.35mm) was 279.5 μW at the emission peak wavelength λ_p = 0.95 μm and 30.2 μW at λ = 0.42 μm.

When the interference filter was removed, the monochromator worked as a white light source.

III. Experiments and Results

1. Si-Mo Bonding

A single crystal wafer of silicon was diffusion bonded on a molybdenum substrate without destroying the crystallinity of silicon. Molybdenum was chosen as the substrate because its thermal expansion coefficient matched closely with that of silicon and it was easily machinable. However a small mismatch between the thermal expansion coefficients of silicon single crystal and molybdenum[6] necessitated an extreme care during temperature cycling after the bond was accomplished. Figure 5 shows the photograph of a silicon wafer bonded on a molybdenum base. A scanning electron microscope view of the bonded edge is shown in Figure 6. In the figure, the grey sponge-like area is silicon, and the lighter area with many wavy lines is the molybdenum surface. Notice that the boundary between the two areas does not show any detectable gap at nearly 10,000 magnification despite the fact that the molybdenum surface is not mirror smooth. The micrograph also shows no sign of alloying between silicon and molybdenum. The bonding was accomplished by diffusion of silicon into molybdenum as an electron beam microprobe analysis indicated.

To prepare for the final bonding, an approximately 7 x 7 x 0.25mm^3 size silicon wafer, polished on one side, was first boiled in acetone, then dipped in HF for 10 seconds prior to the final rinse in deionized water. The molybdenum was carefully machined to insure its surface flatness and treated anodically in concentrated H_2SO_4 followed by 20 minutes of boiling in deionized water.

To bond the silicon to the molybdenum, the unpolished side of the silicon wafer was laid on top of the molybdenum block, and the block was heated to 1100-1200°C by electron beam bombardment in an oil diffusion-pump vacuum system whose pressure during the bonding was at about 1.3 x 10^{-4} N/m^2 (10^{-6}Torr). The bonding initiated at one point, which became brighter than the rest of the silicon surface, and the bright area increased as the bonding spread over

the entire surface in about 15 minutes. A slight pressure, barely enough to hold the wafer in place was helpful in initiating the bond. To avoid the cracking of crystal during the cooling period, a cooling rate of less than 10°C per minute was necessary.

A further development of this technique is considered necessary to produce more reliable bonding of silicon.

2. Surface Activation

The activation procedure described in the literature[4] was adapted for our experiment. After the pressure in the test vehicle stabilized in the 10^{-8} N/m^2 ($\sim 10^{-10}$ Torr) range, the silicon surface was sputter cleaned by argon ion bombardment (1 mA/cm^2, 15 minutes at 600-700 volts) and subsequently anealed at 1000°C for about an hour. The ion bombardment was achieved by connecting a floating d.c. high voltage power supply across the mesh electrodes and the collector electrode. During the anealing, which lasted several hours, the pressure inside the test vehicle rose to 10^{-6} - 10^{-6} N/m^2. The pressure rise was mainly due to the heating of the chamber wall and other parts. After the collector was cooled to nearly room temperature, the cesium valve was open to the cesium reservoir which was kept at 65°C. During the cesiation, the white light from the monochromator was introduced on the collector and photoemission from it was continuously monitored. The surface was slightly over cesiated at first (more than one monolayer coverage), and oxygen was added afterward to complete the activation. The progress of activation monitored by the photoemission current is shown in Figure 7.

It was noted that when the collector was treated only with cesium, the surface work function showed very poor stability even at room temperatures. The photoemission would decrease to about 10% of the original value within 10-20 minutes after the cesium beam was shut off. But when the oxygen treatment was given immediately following the cesiation, the surface maintained its low work function for several days without an appreciable degradation in photoemission. After a prolonged period ($\sim$1 month), the photoemission decreased but

could be restored easily by heating it slightly (50~100°C) and adding small amounts of cesium on the surface.

3. Work Function Measurements

The work function of the activated surface was measured by three different methods: (i) Spectral photoemission measurements, (ii) I-V characteristics and (iii) Thermionic emission.

During the activation process, the continuous lowering of the work function was monitored by white light photoemission which rapidly increased as the work function decreased. At the end of each activation process, the spectral photoemission measurements were conducted to determine the work function of the activated surface. In Figure 8, the results of such measurement are shown for an n-type and a p-type samples. The work function of the n-type Si was less than 1.2 eV as the curve indicates and it was estimated to be 1.0 eV considering the fact that the curve could have been extended if appropriate filters had been available. The work function of the p-type sample was determined to be 1.35 eV from the knee of the curve.

After the activation was completed, I-V characteristics were used to determine the difference of the work functions of collector and emitter. Therefore, if the work function of one electrode is known, the work function of the other is determined.

In our experiments, the white light photoemission current from the sample collector was used as the source of current. The emitter (not heated) and the grid (with bias voltage Vg) both were used as the collector of photo electron current from the sample collector electrode. The circuit for this measurement is shown in Figure 9. This method produced two sharp knees "a" and "b" (Figure 10). The work function of grid, which was fully cesiated during the cesiation of the collector, was determined to be 1.65eV from its spectral photoemission threshold. Knowing the work function of the grid, the collector work function is determined from the relation:

$$\phi_c = \phi_g + V_g - V_a \qquad (1)$$

where V_a is the voltage at the saturation current knee "a" in Figure 10, V_g is the grid bias voltage, ϕ_c and ϕ_g are collector and grid work functions respectively. Similarly, the voltage V_b at "b" is related to the collector work function by the equation:

$$\phi_c = \phi_e - V_b \tag{2}$$

In this equation, however, the emitter work function ϕ_e was not predetermined because the work function of the bare tungsten is too high to induce photo-emission by the visible spectrum light source. Instead the collector work function determined from equation (1) was used to derive the emitter work function to gain confidence in the measurements. The emitter work function determined by equation (2) was 4.65eV.

Considering the fact that the emitter is a polycrystalline tungsten and the surface might be covered with thin oxide layer, the value $\phi_e = 4.65$eV is very reasonable. And for each measurement, the voltage separation between the points "a" and "b" were examined, because it is independent of ϕ_c and remains constant as long as ϕ_e and ϕ_g stay unchanged, as shown by the relation,

$$V_b - V_a = (\phi_e - \phi_g) + V_g \tag{3}$$

which can be readily obtained from equations (1) and (2).

The accuracies of these measurements are considered to be within $\pm$0.05eV. The uncertainty arises mostly from the uncertainty in determining the precise position of the "knee."

When the thermionic emission became considerable at elevated temperatures, the work function ϕ was computed from the Richardson equation:

$$\phi = -\frac{kT}{e} \ln \frac{J}{AT^2} .$$

The value of 120 $A/cm^2-°K^2$ was used for the Richardson constant A. We have not made any attempt to obtain an exact value of A for silicon or make a distinction between n- and p-types. However, according to Martinelli[8] the thermionic emission properties of activated n- and p-type silicon surfaces were identical. This was explained by noting that most of the thermionic emission originated from the activated surface layer rather than the bulk material. The work function measured by this method and by the I-V characteristics agreed very well where both methods were applied.

The leakage currents had to be discriminated very carefully for thermionic emission measurements because the leakage increased rapidly as the collector temperature and the cesium arrival rate increased. Figure 11 shows the thermionic emission current from the collector as a function of the collecting electrode mesh voltage. The curve shows a definite slope due to the leakage currents. In this figure, the leakage can be discriminated by extrapolating the portion of saturation current to the voltage zero axis, which gives the zero field saturation current, I_o from which the current density J was determined. In actual experiments the leakages were discriminated by measuring the currents at two different voltages, 23V and 47V (see Figure 12) for all measurements. The zero field saturation current I_o was then calculated from the following relation,

$$I_o = GV_{23} - I_{23} , \qquad (4)$$

where

$$G = \frac{I_{23} - I_{47}}{V_{23} - V_{47}}$$

subscripts 23 and 47 identify two values measured at corresponding voltages.

The results of the work function measurements from the activated silicon collectors are summarized in Table II.

Table II. Work Functions of the Activated Silicon Collectors

Collector Identification	Work Function ϕ_c, eV	Remarks
Si (n) #1	---	Si Cracked during anealing
Si (n) #2	1.0 (Initial result)	Spectral photoemission, I-V characteristics
	1.2 (Subsequent results)	ϕ_c vs T/T_{Cs} was determined, Si became unbonded from Mo.
Si (n) #3	---	Thermocouple failed and Si cracked.
Si (n) #4	1.2	Successful ϕ_c vs T/T_{Cs} plot obtained.
Si (p) #5	---	Bonding failure.
Si (p) #6	1.35	Successful ϕ_c vs T/T_{Cs} plot

As the table shows, a collector work function as low as 1.0eV has been achieved. The value agrees with the reported work function of activated silicon (100) surface[5, 7, 8]. However, in our test vehicle, which was made to simulate a thermionic converter, a work function of 1.2eV was more frequently obtained. The Si (p) #6 sample shows a work function of 1.35eV. Because of repeated pumping on Cs vapor, which made the ion pump inefficient, the #6 collector was activated when the pressure in the test vehicle was in the order of 10^{-5} N/m^2 ($\sim 10^{-7}$ Torr).

4. Work Function Variation With Respect to Temperature

During the experiments the collector temperature, T_c, was measured by a W(5%), Re - W (26%), Re thermocouple. The spot welded tip of the thermocouple was inserted in a thermocouple well drilled into the molybdenum body approximately 1mm below the surface of the Si wafer. The collector heating was accomplished by electron bombardment during the anealing at 1000°C, and by radiation heating during the work function variation measurements at high

collector temperatures. The radiation heating could bring the collector temperature up to 500°C. During the radiation heating, the heater filament was biased positively with respect to the collector so that no electrons from the heater could arrive at the collector.

The equivalent cesium temperature, T_{Cs}, which determines the equilibrium cesium arrival rate on the collector surface was determined as follows: First, the temperature T'_{Cs} of the reservoir, was measured by a chromel-alumel thermocouple which was attached to the tip of the reservoir using high thermal conductivity epoxy. Then the cesium molecular flux on the Si surface was computed by using the vapor pressure data of cesium and by calculating the conductance of the 25cm long tubing, which separated the reservoir and the Si surface. Finally, the equivalent cesium temperature T_{Cs} which produces this arrival rate was determined by using the vapor pressure data again. To avoid any condensation of Cs on the transporting tube wall, the temperature of the tubing was kept higher than the Cs reservoir at all times during experiments. The result of this computation was plotted in Figure 13. From this curve, the measured cesium temperature T'_{Cs} was readily converted to an effective Cs temperature T_{Cs}. An experimental verification of this correlation was accomplished during the activation procedure. Assuming the sticking coefficient of cesium on Si is unity at sub-monolayer coverage, the time it takes to activate the Si can be converted to the Cs vapor temperature by correlating it with the arrival rate of Cs atoms. The agreement between the calculated values (Figure 13) and the experimentally derived values was excellent. If the calculations and the assumptions carried an uncertainty factor of 2 in the arrival rates, the resulting temperature uncertainty is 10 degrees at 300°K, and 20 degrees at 470°K, less than 5%.

Figure 14 shows the results of the work function measurements at elevated collector temperatures. These curves are plotted in the form of Rasor-Warner plots using an effective cesium temperature T_{Cs}. Curve (1) shows the results of an n-type collector (Si (n) #4) which had been activated to 1.2eV, curve (2) shows the results from a p-type collector (Si (p) #6) which had been activated to 1.35eV and curve (3) for tungsten polycrystalline surface for comparison purposes. Table III shows the parameters associated with these curves.

Table III. Parameters Associated with ϕ vs. T/TCs Measurements

Curve #	Identification	Temperature Range	Highest Temperature for Lowest ϕ
(1)	Si (n) #4	$311°K \leq Tc \leq 812°K$ $278°K \leq TCs \leq 335°K$	$Tc = 409°K$ $TCs = 326°K$
(2)	Si (p) #6	$499°K \leq Tc \leq 829°K$ $288°K \leq TCs \leq 410°K$	$Tc = 555°K$ $TCs = 410°K$

Within the temperature range of our experiments, the curves follow the pattern of the Rasor-Warner curves except that lower minimum work function is achieved at lower T/T_{Cs} value than with tungsten. The shape of curves suggests that the work function variation is controlled by the balance between the thermal desorption of cesium from, and the arrival to the surface. However, our results are in disagreement with the reported observation by Goldstein[5] who observed that the thermal desorption of cesium did not take place until the silicon was heated to 700°K.

It is noted that the minimum work functions in the figure are appoximately the same as the originally activated values. The return of the work functions to their initial values even after the heating to higher than 800°K suggests that the adsorbed oxygen stays intact on the surface at these temperatures. In fact Goldstein[5] reported that the oxygen adsorbed on silicon remained intact up to nearly 1000°K. Therefore, his result is in agreement with our observations with respect to oxygen effects.

Figure 14 also shows work function difference of 0.2-0.3eV between the curves (1) and (2) at high T/T_{Cs} values. Although the reason for the difference is not known at this time, the difference might be due to differences of dopants in two samples, and also in the details of the activation processes.

IV. Conclusions

The surface of several (100) oriented single crystal silicon wafers, which were diffusion bonded to a molybdenum substrate, was successfully activated to achieve work functions desirable for thermionic collector electrodes at low temperatures. The activation of sample electrodes was made in a simulated thermionic converter using beams of cesium and oxygen. The degree of activation was determined from the photo-electron emission measurements performed with the electrode at room temperature. The lowest work function of 1.0 eV was achieved with an n-type silicon sample. In contrast a p-type silicon achieved a lowest work function of 1.35 eV according to the photoemission yield threshold, although the net photo emission was larger with p-type than with n-type. The work function of 1.35 eV should not be considered to be the representative value for an activated p-type silicon since the cleanliness of the test vehicle was somewhat in doubt during this activation. Also it was found that work function between 1.2 and 1.4 eV can be readily obtained regardless of the sample type (n or p), without requiring rigorous activation procedures.

The stability of activated surfaces was determined by measuring surface work functions at elevated temperatures up to 829°K. Since the purpose of this experiment was to determine the ability of such surfaces in maintaining low work functions at elevated temperatures by replenishing the desorbing cesium using an increased arrival of cesium atoms, the work function was measured as a function of T/T_{Cs} in which T_{Cs} was calculated from the cesium arrival rate. The results indicated that the same work function could be achieved at an elevated temperature T as long as T/T_{Cs} was kept constant by proportionately increasing T_{Cs}. Thus the relationship between the work function ϕ and T/T_{Cs} was found analogus to that of metal.

Acknowledgements

The authors acknowledge Mr. Michael Donovan for his contributions in achieving a successful Si-Mo bonding, and Tom Osheroff for his suggestions on the monochromator designs.

References

1. N. S. Rasor, Proceedings of Third International Conference on Thermionic Electric Power Generation, Jülich, P. 1027, June 1972.

2. V. S. Fomenko, Edited by G. V. Samsonov, Handbook of Thermionic Properties, Plenum Press Data Division, (1966).

3. Alleau, T. and Bacal, M. "Influence of Oxygen Adsorption and Oxygen-Cesium Co-adsorption on (100) Tungsten Work Function," Report of Thermionic Conversion Specialist Conf., P. 434, Miami, Fla., (1970).

4. A. H. Sommer, "Photoemissive Materials, Preparation, Properties and Uses," Wiley, New York, (1968).

5. Bernard, "LEED, Auger and Plasmon Studies of Negative Electron Affinity on Silicon produced by the Adsorption of Cs and O." Surf. Sci. 35 227, (1973).

6. G. A. Slack and S. F. Bartram, "Thermal Expansion of Some Diamondlike Crystals," J. Appl. Phys., Vol. 46, No. 1, 89 (1975).

7. R. V. Martinelli, "Negative Electron Affinity Surfaces on Silicon Using a Rubidium/Oxygen Dipole Layer," J. Appl. Phys., Vol. 44, 2566, (1973).

8. R. V. Martinelli, "Thermionic Emission From the Si/Cs/O (100) Surface," J. Appl. Phys., Vol. 45, No. 3, 1183 (1974).

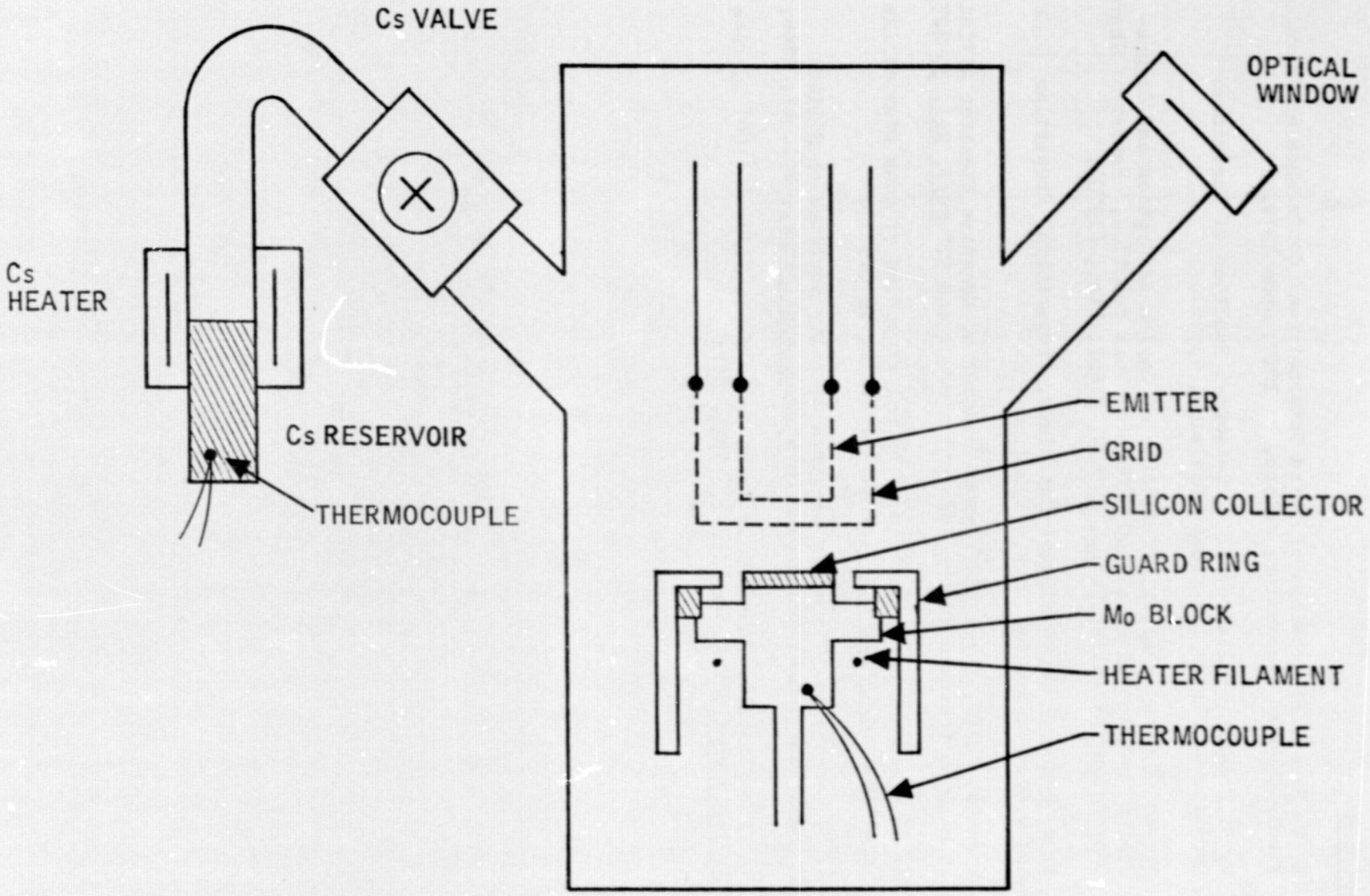

Figure 1. Schematic Drawing of the Test Vehicle

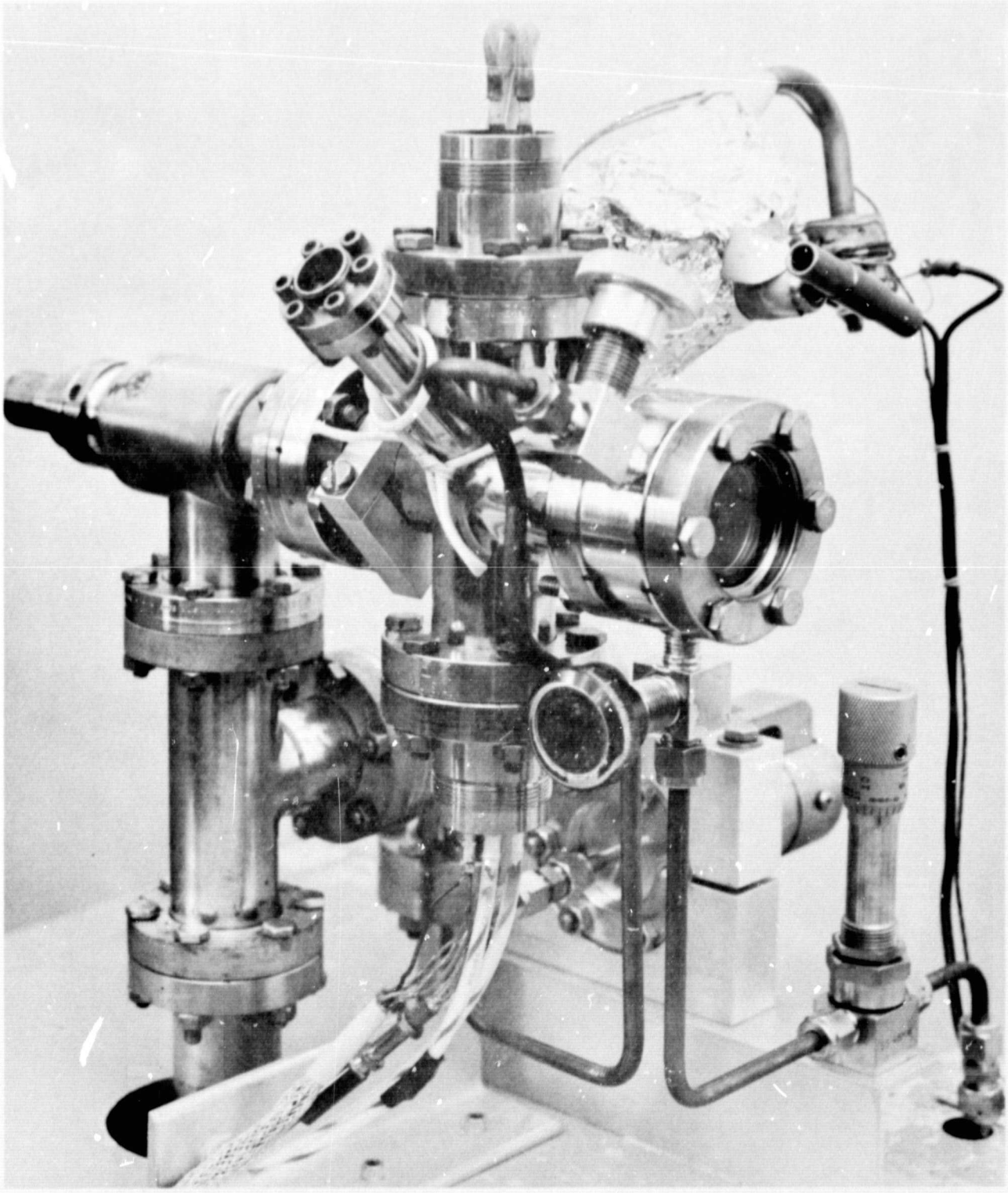

Figure 2. Test Set-up Photograph.

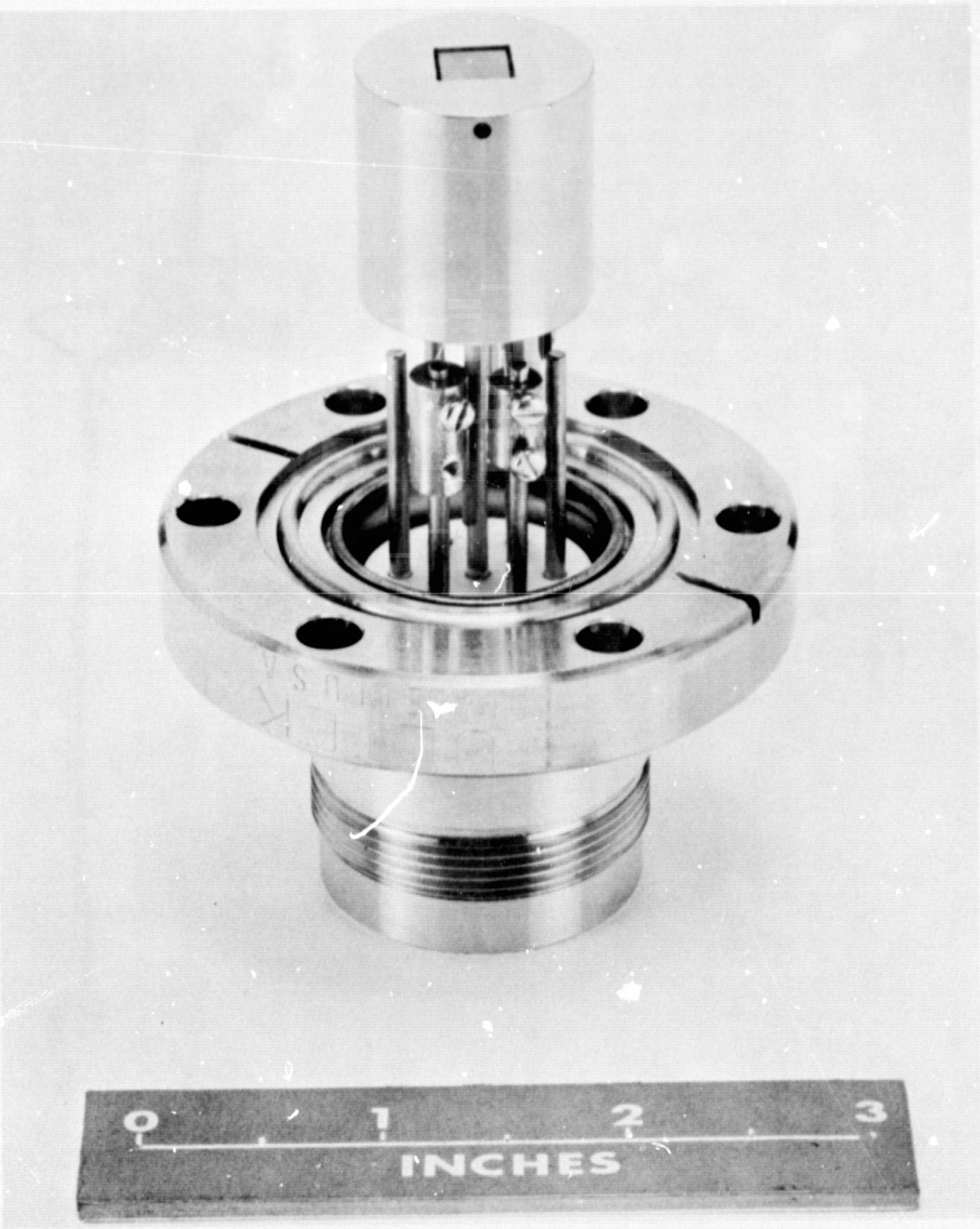

Figure 3. Collector Assembly.

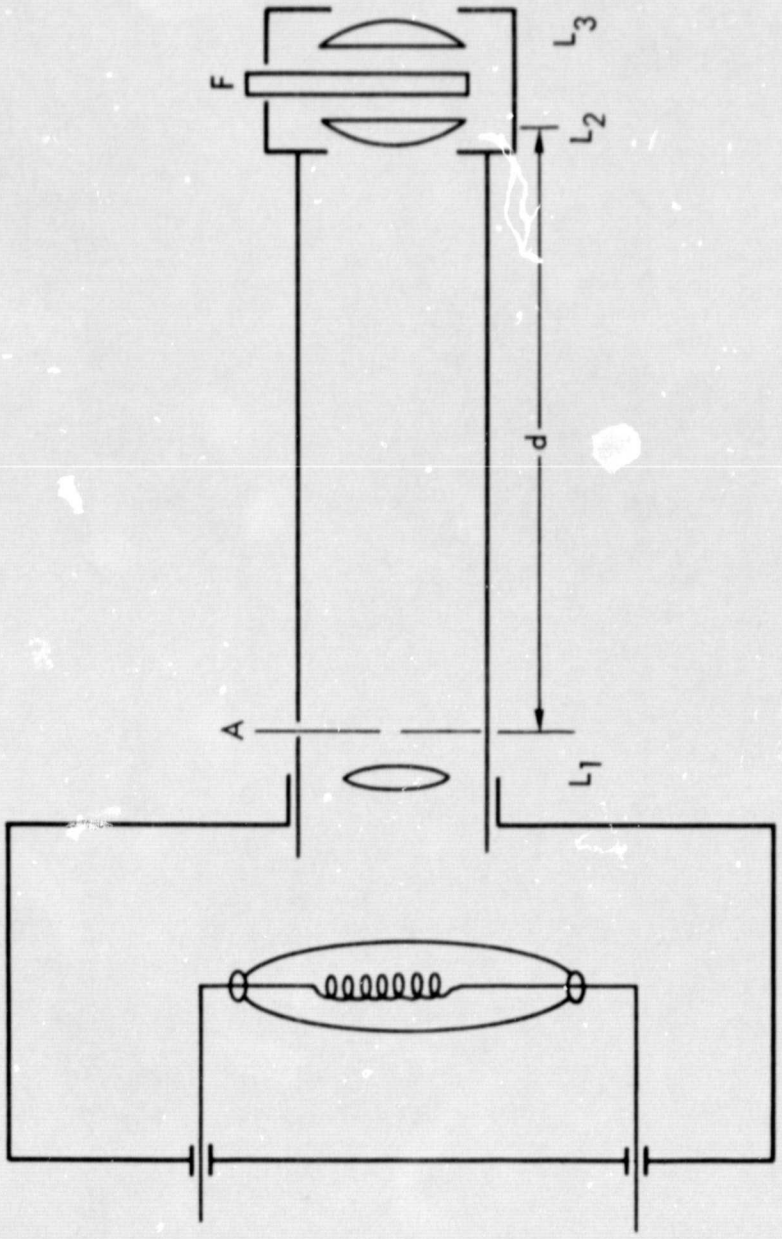

Figure 4. Schematic Drawing of Optical Monochromator.

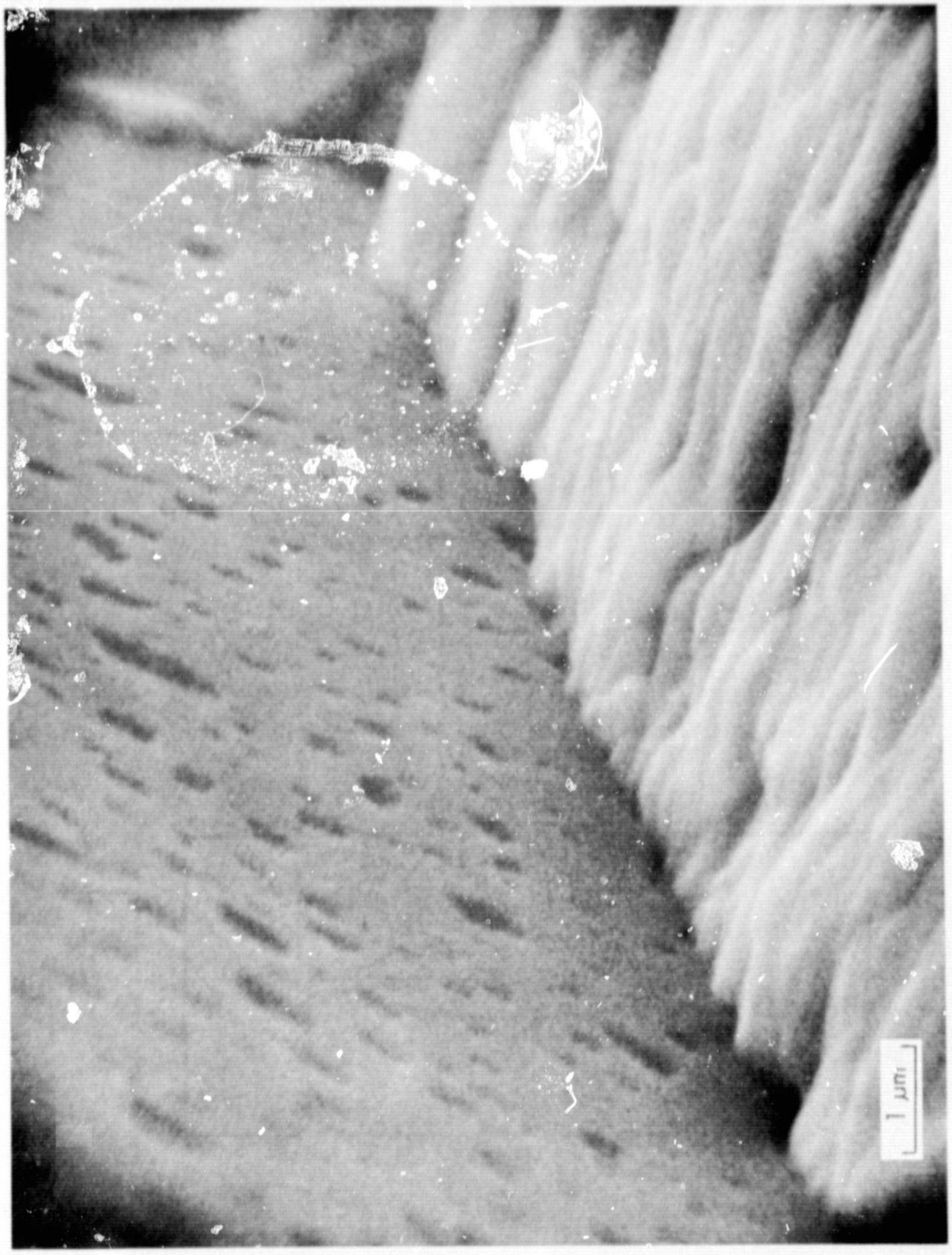

Figure 5. Silicon Wafer Bonded on Molybdenum Base.

ORIGINAL PAGE IS
OF POOR QUALITY

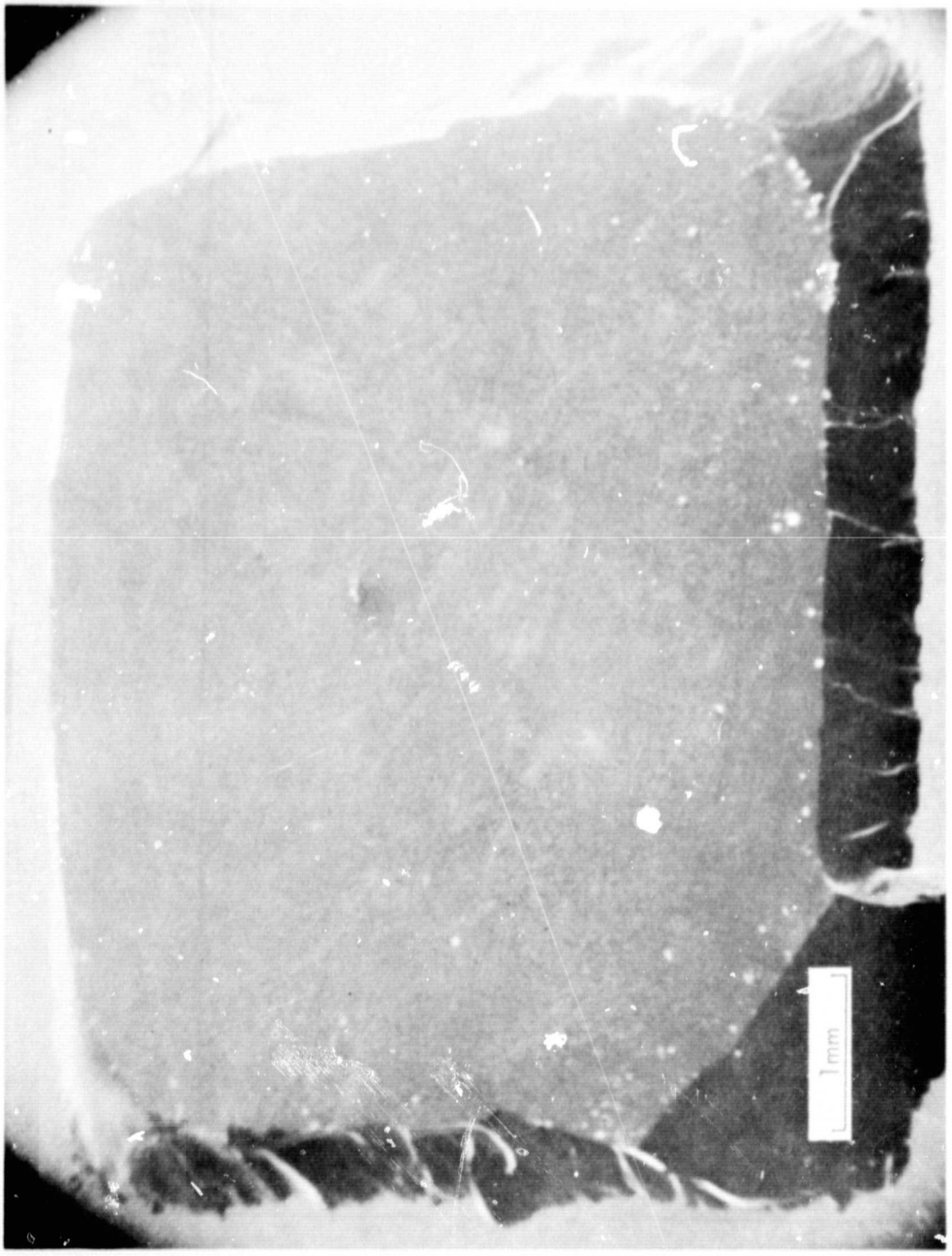

Figure 6. SEM Micrograph of the Bonded Region.

ORIGINAL PAGE IS
OF POOR QUALITY

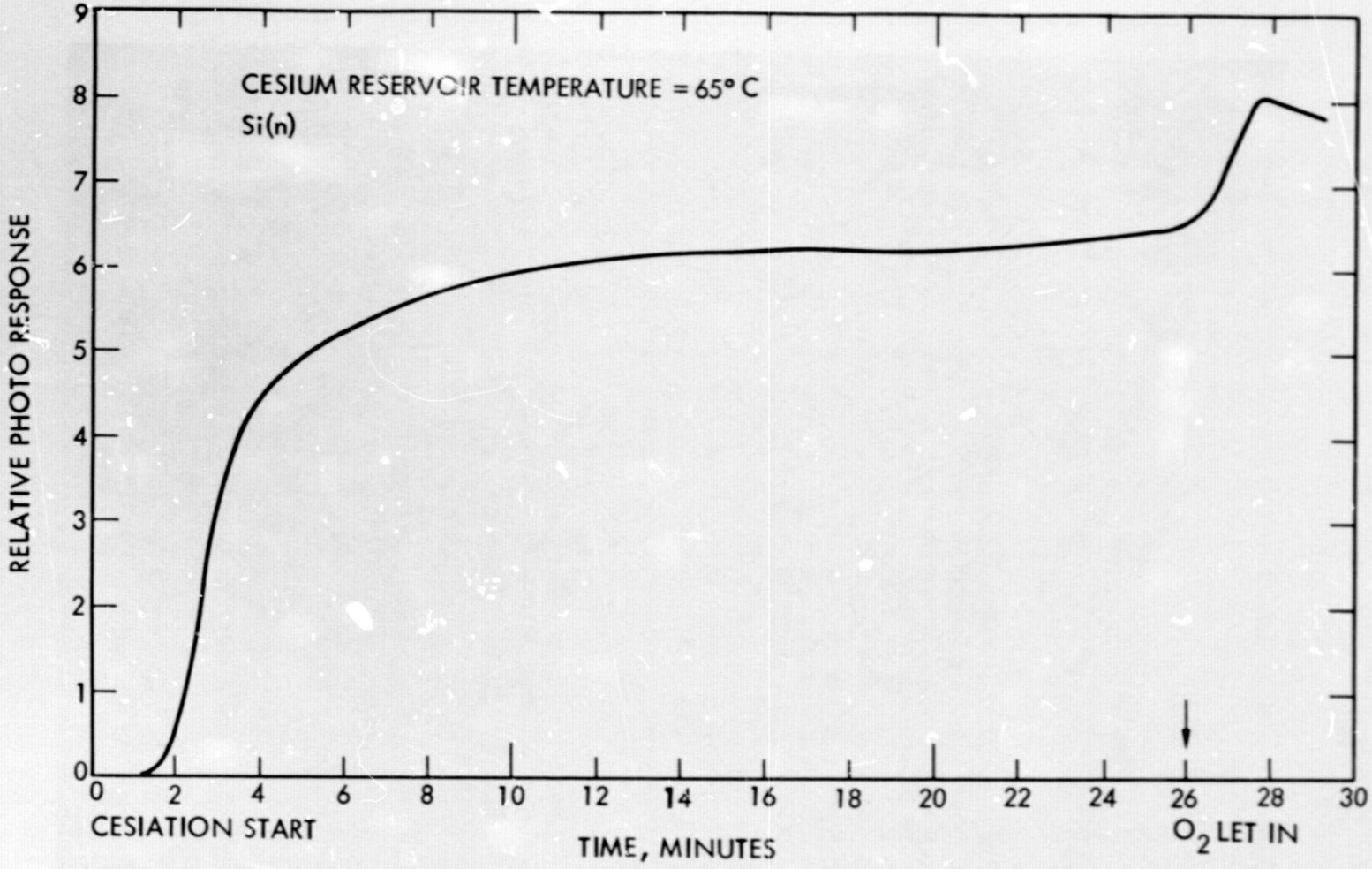

Figure 7. Photoemission During Activation.

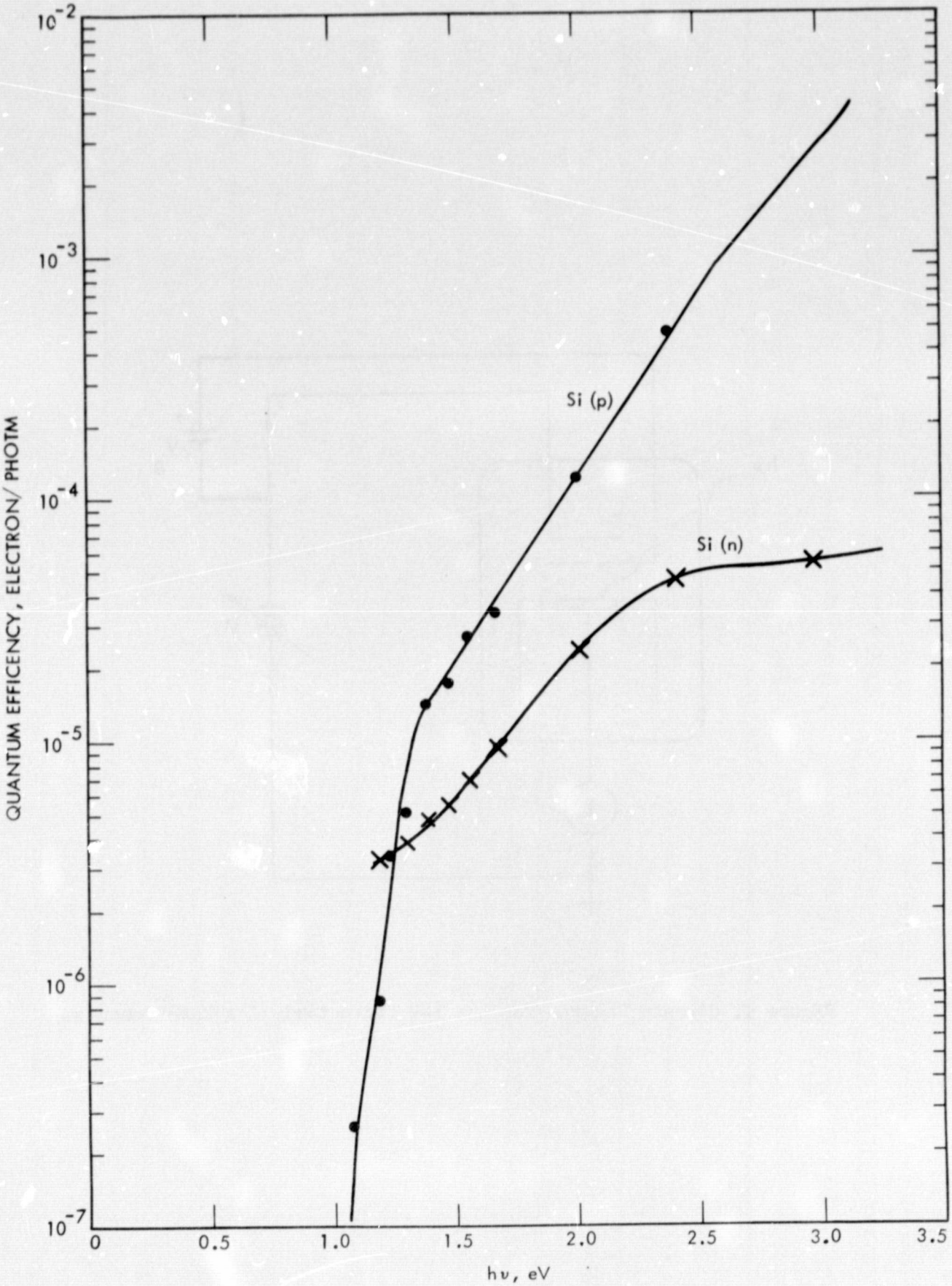

Figure 5. Spectral Photoemission Quantum Efficiencies.

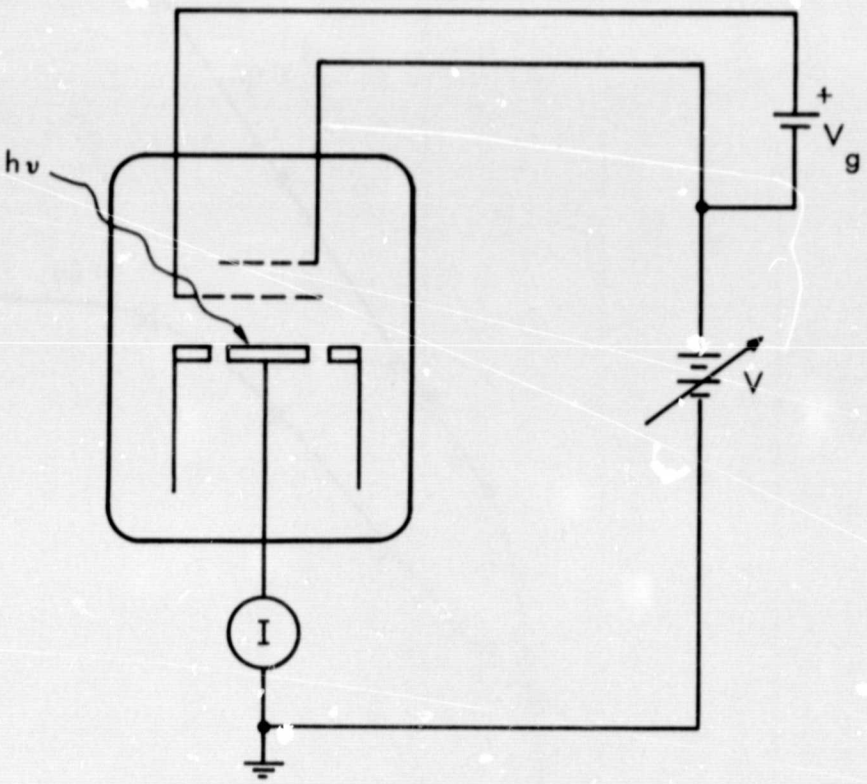

Figure 9. Circuit Diagram for the I-V Characteristics Measurements.

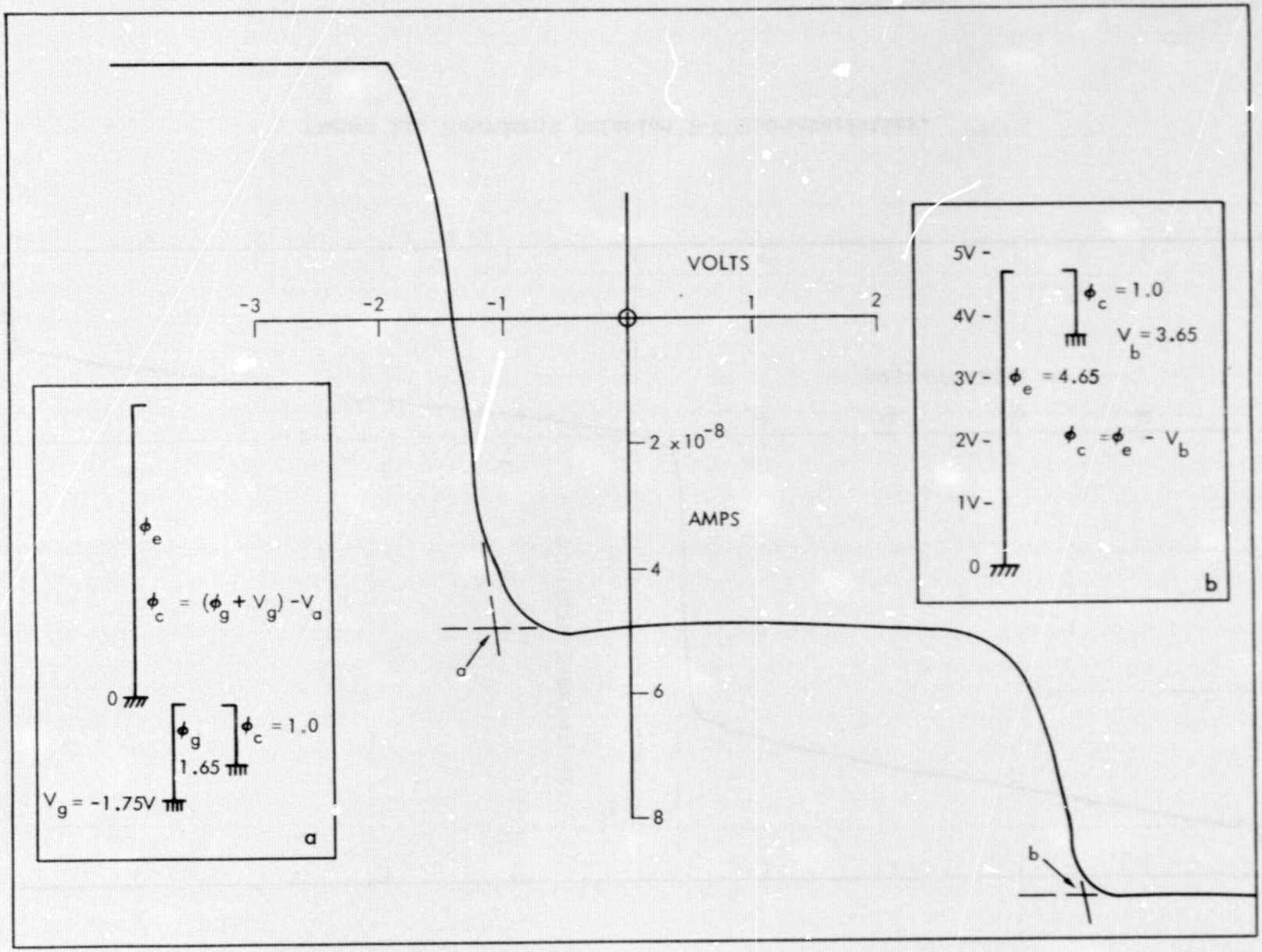

Figure 10. Photoemission I-V Characteristics.

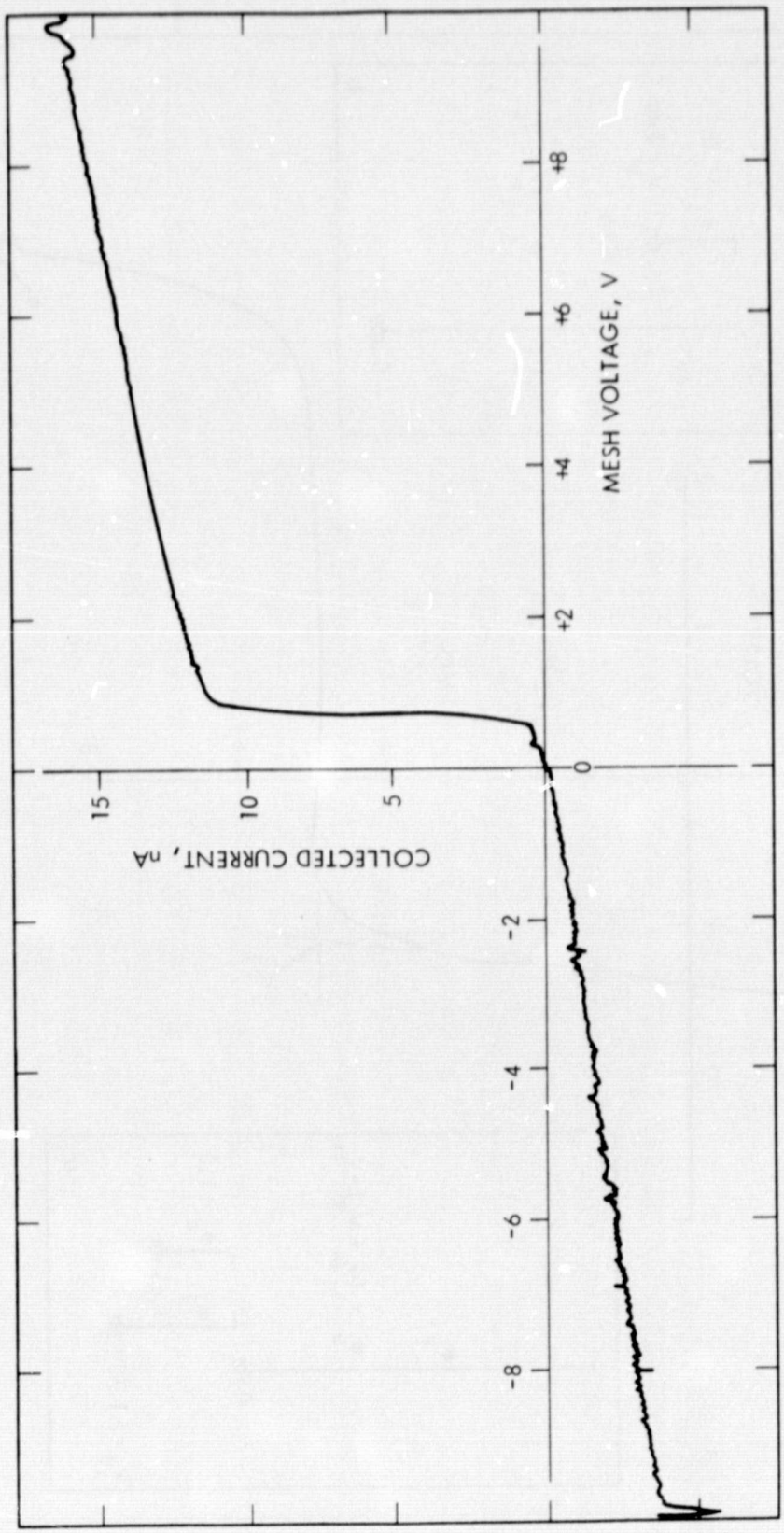

Figure 11. Thermionic Emission I-V Characteristics.

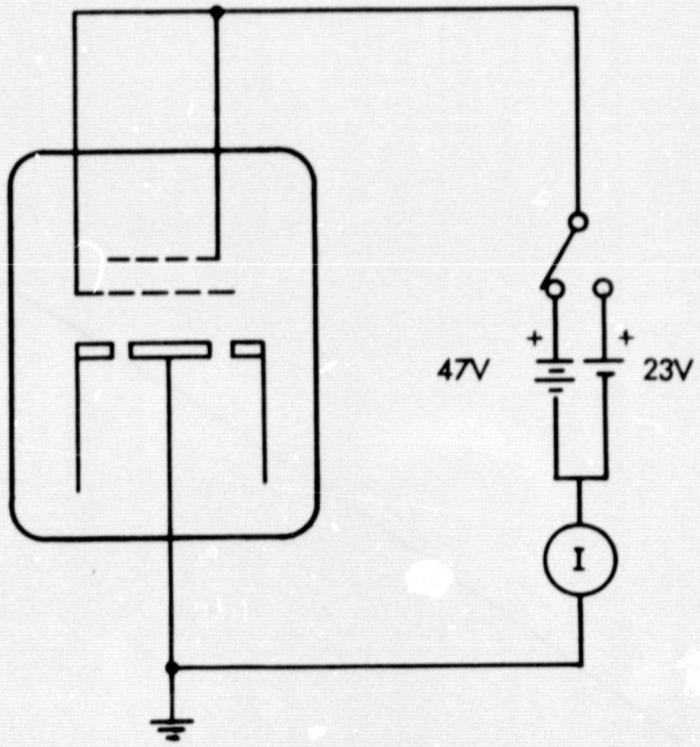

Figure 12. Circuit for Thermionic Emission Measurements.

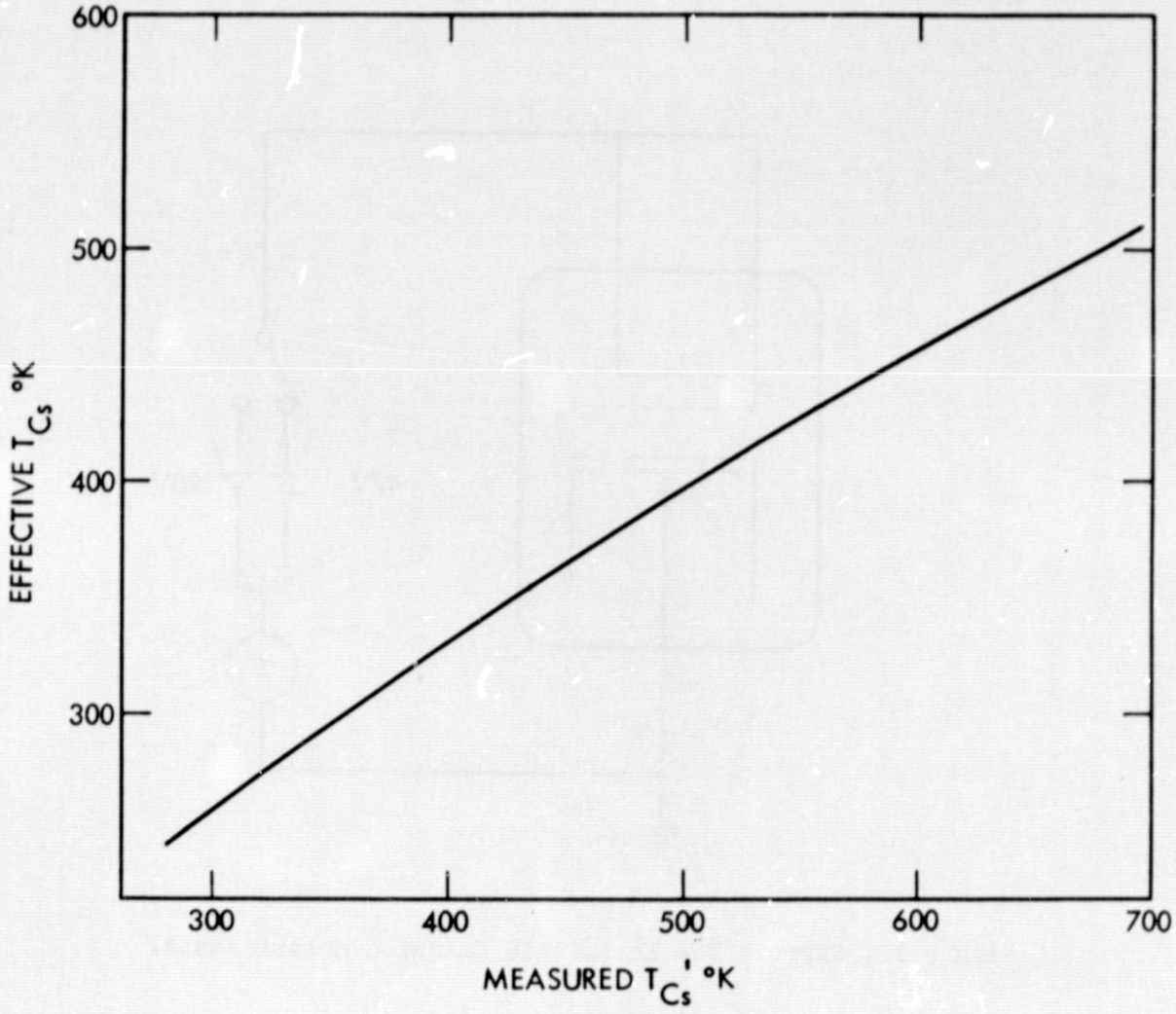

13. Effective Cs Vapor Temperature vs. Reservoir Temperature.

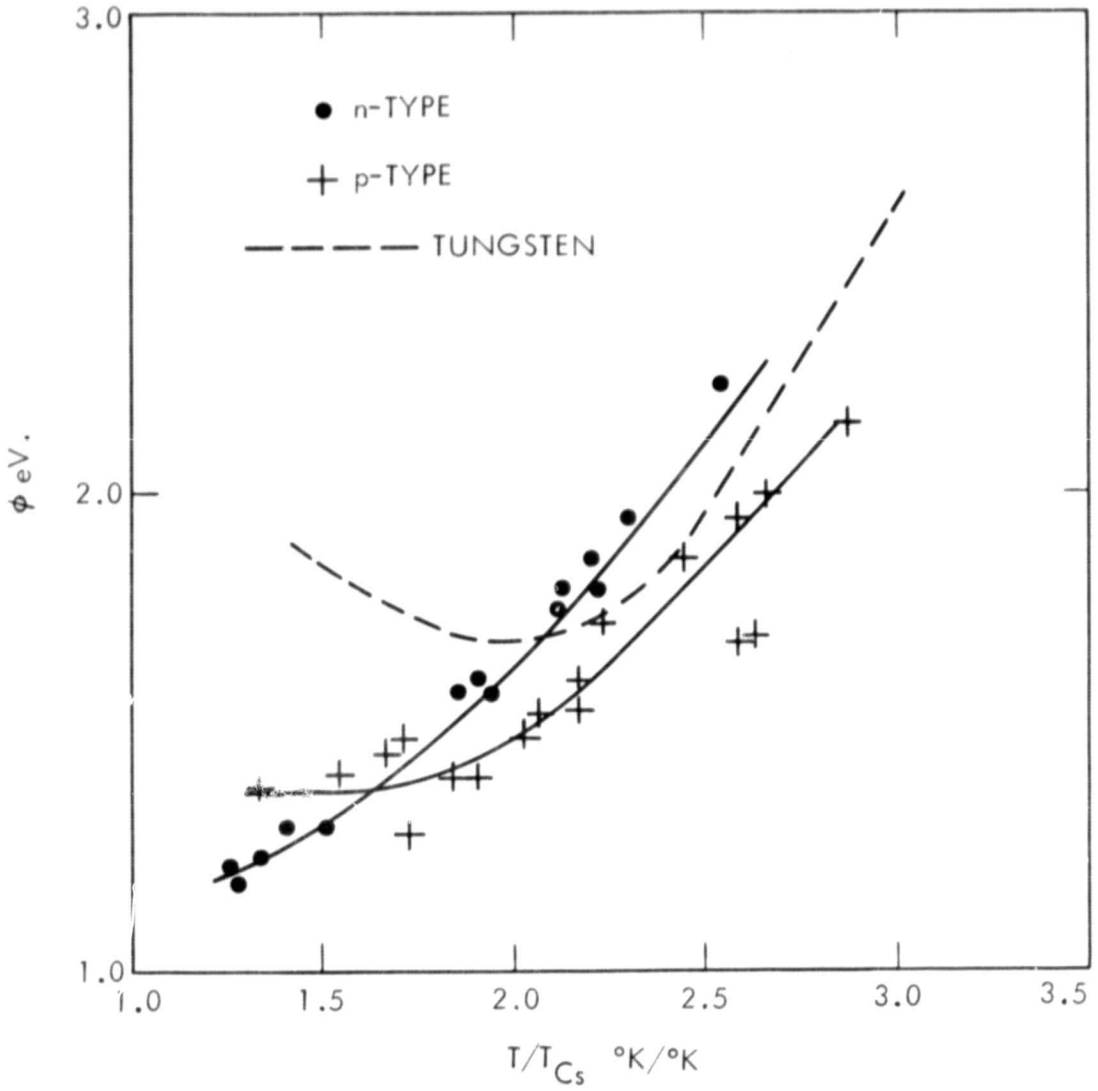

Figure 14. Collector Work Function vs. T/Tcs.